

A Reformulated Three-Layer Sea Ice Model

MICHAEL WINTON

NOAA/Geophysical Fluid Dynamics Laboratory, Princeton, New Jersey

(Manuscript received 21 December 1998, in final form 28 June 1999)

ABSTRACT

A model is presented that provides an efficient approximation to sea ice thermodynamics for climate studies. Semtner's three-layer framework is used, but the brine content of the upper ice is represented with a variable heat capacity as is done in more physically based models. A noniterative fully implicit time-stepping scheme is used for calculation of ice temperature. The results of the new model are compared to those of Semtner's original model.

1. Introduction

A sea ice model, in general, may contain subcomponents treating 1) dynamics (ice motion), 2) ice transport, 3) multiple ice thickness categories (including leads), 4) surface albedo, and 5) vertical thermodynamics. This paper is concerned with a scheme for the last of these processes. Hibler and Flato (1992) introduce many aspects of sea ice modeling and Ebert and Curry (1993) discuss the details of surface albedo representation.

At issue in the vertical thermodynamics part of an ice model are the vertical resolution in the ice and snow, and the representation of their conductivities, light transmission, and heat capacities including the latent heat of brine inclusions. Bitz et al. (1996) and Battisti et al. (1997) discuss the impact of snow and vertical resolution in the ice upon the representation of natural thickness variability. Thermodynamic models with a range of sophistications have been devised to represent sea ice in climate models. The simplest are fixed- or zero-heat-capacity slab models and the most sophisticated are multilayer models with ice properties dependent upon temperature and salinity. Semtner (1976) found that an intermediate model with one snow layer and two ice layers using constant heat conductivities and a simple parameterization of the brine content was able to mimic the seasonal cycle of the sophisticated multilayer model of Maykut and Untersteiner (1971).

The treatment of the brine content of the ice is one demarcating feature distinguishing simple and sophisticated models. Since sea ice contains salt, it also con-

tains an amount of liquid water needed to dilute its salt to a brine with freezing temperature equal to the sea ice temperature. Thus, as the ice is heated, for example, two changes occur: 1) the temperature of the ice and its brine increases, and 2) the higher temperature allows for a more dilute brine and so some ice melts, increasing the brine content of the ice. Consequently, sea ice conserves an enthalpy, E , per unit mass having the form (Bitz and Lipscomb 1999; Ono 1967)

$$E(T, S) \equiv C(T + \mu S) - L(1 + \mu S/T), \quad (1)$$

where C , L , S , and T are the heat capacity, latent heat of fusion, salinity and temperature of the ice, respectively, and μ is a constant equal to minus the freezing temperature (in °C) divided by the salinity. From (1) conservation of enthalpy for a mass, m , of ice can be written in the variable heat capacity form:

$$m \frac{dE}{dt} = m \left(C + \frac{L\mu S}{T^2} \right) \frac{dT}{dt} = F, \quad (2)$$

where F is the heating of the ice.

Equation (2) poses a numerical difficulty—for while it is desirable to solve the ice temperature equation implicitly in order to avoid small time steps when the ice is thin, the variable heat capacity form of the equation, in general, requires that an iterative technique be used for multiple ice layers coupled by diffusion. Semtner sought to represent the brine content of the ice by a parameterization that avoided time stepping (2). A certain fraction of the solar radiation impinging upon the ice was stored in a brine pocket variable that released energy to the upper half of the ice under cooling conditions, maintaining its temperature at 0°C until the brine energy was exhausted. This parameterization achieves

Corresponding author address: Dr. Michael Winton, GFDL/NOAA, P.O. Box 308, Princeton, NJ 08542.
E-mail: mw@gfdl.gov

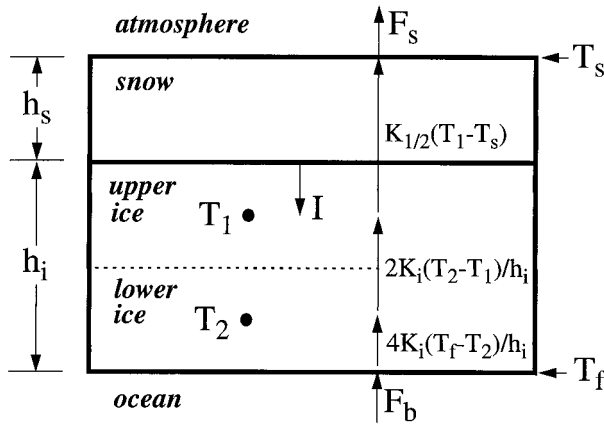


FIG. 1. Schematic representation of the three-layer model. The model has four prognostic variables: h_s , h_i , T_1 , and T_2 . The temperature of the bottom of the ice is fixed at T_f , the freezing temperature of seawater. The temperature of the top of the ice or snow, T_s , is determined from the surface energy balance.

computational economy at the expense of decoupling the ice temperature from its brine content.

This paper presents a model that retains the layer structure of the Semtner model but treats the upper half of the ice as a variable heat capacity layer as in the more sophisticated models of Bitz and Lipscomb (1999), Ebert and Curry (1993), and Maykut and Untersteiner (1971). In this way, the brine reservoir is treated more physically and naturally than in Semtner's model without an increase in computational expense. In particular, the new model follows the practice, advocated by Bitz and Lipscomb, of using $-E$ as the energy needed for melting surface ice. They point out that this avoids double counting the melting of brine contained in the ice when ice melts at the surface. Thus, the reduction in brine that accompanies surface melting is automatically handled in the new model while it is ignored in the Semtner model. By accounting for sensible heat in the melting energy for both layers, the new model also avoids a small source of energy nonconservation found in the Semtner model (Bitz and Lipscomb 1999). A further advantage of the new model is that it is fully implicit, eliminating the need to switch to a zero-heat-capacity model when the ice becomes thin, as is typically done with the Semtner model. The next section presents the physical and numerical formulation of the new model. In the following section, results of the new model are compared with those of Semtner's model. Conclusions are presented in the final section.

2. The model

The model consists of a zero-heat-capacity snow layer overlying two equally thick sea ice layers (Fig. 1). The upper ice layer has a variable heat capacity to represent

brine pockets. The lower ice layer has a fixed heat capacity. The prognostic variables are h_s , the snow layer thickness; h_i , the ice layer thickness; and T_1 and T_2 , the upper and lower ice layer temperatures located at the midpoints of the layers $h_i/4$ and $3h_i/4$ below the ice surface, respectively.

Two of the prognostic variables of Semtner's model have been eliminated: the brine content of the upper ice and the snow temperature. A separate brine variable is no longer needed because the brine content in the new model is completely determined by the upper ice temperature and the (predetermined) ice salinity. The heat capacity of the snow layer is typically small relative that of the ice. In regions where snowfall is large, the depth of the snow layer relative to the ice is limited by snow-to-ice conversion taking place as seawater floods snow below the waterline. It has been estimated that 8% of sea ice in the Weddell Sea is formed through this process (Eicken et al. 1995). If all snow below the waterline is converted to sea ice, snow can represent at most $1 - \rho_i/\rho_w \approx 0.1$ of the sensible heat capacity of the snow-ice system. When latent heat capacity is also considered this ratio becomes even smaller since snow is fresh and does not form brine inclusions. For these reasons snow layer heat capacity has been neglected in the new model.

The ice model performs two functions. The first is to calculate the ice temperature and the second is to calculate changes in the thickness of ice and snow. In an atmosphere-ice model, the temperature calculation is typically done at each atmospheric physics time step, so that the surface temperature can be used as a boundary condition for vertical mixing. It is therefore desirable that this computation be as efficient as possible.

a. Ice temperature calculation

The surface temperature is determined from the diagnostic balance between the upward conduction of heat through snow and/or ice and upward flux of heat from the surface F_s . For this purpose we employ an expression for F_s that is linearized about the surface temperature at the last time step, \hat{T}_s :

$$F_s(T_s) = F_s(\hat{T}_s) + \frac{\partial F_s(\hat{T}_s)}{\partial T_s}(T_s - \hat{T}_s). \quad (3)$$

Here $F_s(\hat{T}_s)$ and $\partial[F_s(\hat{T}_s)]/\partial T_s$ would typically be calculated using downward short- and longwave radiative fluxes, bulk formulas for latent and sensible heat fluxes, the Stefan-Boltzmann formula for the upward longwave, and the computed surface albedo for the upward shortwave. This part of the calculation is unchanged from Semtner (1976).

The conductive flux to the surface is

$$K_{1/2}(T_1 - T_s), \quad (4)$$

where

TABLE 1. Notation.

Symbol	Definition	Value
ρ_i	Density of ice	905 kg m ⁻³
ρ_s	Density of snow	330 kg m ⁻³
C	Ice heat capacity (excluding internal melt)	2100 J kg ⁻¹
L	Latent heat of freezing	334×10^3 J kg ⁻¹
K_i	Thermal conductivity of sea ice	2.03 W m ⁻¹ °C ⁻¹
K_s	Thermal conductivity of snow	0.31 W m ⁻¹ °C ⁻¹
μ	Constant relating freezing temperature to salinity	0.054°C per mil.
S	Salinity of sea ice	1 per mil
T_f	Freezing temperature of seawater	-1.8°C
h_s	Snow thickness	Variable (m)
h_i	Ice thickness	Variable (m)
T_1	Temperature of upper half of ice	Variable (°C)
T_2	Temperature of lower half of ice	Variable (°C)

$$K_{1/2} \equiv \frac{4K_i K_s}{K_s h_i + 4K_i h_s} \quad (5)$$

is the effective conductive coupling of the snow–ice layer between the surface and the upper layer ice temperature $h_i/4$ beneath the snow–ice interface. See Table 1 for other symbol definitions. Here $K_{1/2}$ is determined by balancing the conductive flux of heat through the ice to the snow–ice interface with the conductive flux of heat through the snow away from the interface. Notice, that it also applies when $h_s = 0$. As in the Semtner model, the ice conductivity is assumed to be constant rather than a function of temperature and salinity, as it is in more sophisticated models (Maykut and Untersteiner 1971; Bitz and Lipscomb 1999).

Now equating (3) and (4) gives the surface temperature

$$T_s = \frac{K_{1/2} T_1 - A}{K_{1/2} + B}, \quad (6)$$

where we define

$$A \equiv F_s(\hat{T}_s) - \hat{T}_s \frac{\partial F_s(\hat{T}_s)}{\partial T_s} \quad \text{and} \quad (7)$$

$$B \equiv \frac{\partial F_s(\hat{T}_s)}{\partial T_s}. \quad (8)$$

For the upper layer of the ice, (2) is written:

$$\frac{\rho_i h_i}{2} \left(C + \frac{L\mu S}{T_1^2} \right) \frac{dT_1}{dt} = K_{1/2}(T_s - T_1) + K_{3/2}(T_2 - T_1) + I, \quad (9)$$

where I is the surface penetrating solar radiation absorbed by the ice¹ and

$$K_{3/2} \equiv 2K_i/h_i \quad (10)$$

is the conductive coupling between the two ice temperature points. The prognostic ice temperature equation for the fixed heat capacity ice lower layer is

$$\frac{\rho_i h_i}{2} C \frac{dT_2}{dt} = K_{3/2}(T_1 - T_2) + 2K_{3/2}(T_f - T_2). \quad (11)$$

The discrete forms of (9) and (11) are

$$\begin{aligned} \frac{\rho_i h_i}{2\Delta t} \left(C + \frac{L\mu S}{T_1 \hat{T}_1} \right) (T_1 - \hat{T}_1) &= K_{1/2}(T_s - T_1) \\ &+ K_{3/2}(T_2 - T_1) + I \end{aligned} \quad (12)$$

and

$$\begin{aligned} \frac{\rho_i h_i}{2\Delta t} C (T_2 - \hat{T}_2) &= K_{3/2}(T_1 - T_2) \\ &+ 2K_{3/2}(T_f - T_2), \end{aligned} \quad (13)$$

where a hat denotes a value at the previous time step. In deriving the left-hand side of (12) we have used the fact that

$$\int_{\hat{T}}^T \frac{dT'}{T'^2} = \frac{T - \hat{T}}{T \hat{T}}. \quad (14)$$

Solving (13) for T_2 gives

$$T_2 = \frac{2\Delta t K_{3/2} (T_1 + 2T_f) + \rho_i h_i C \hat{T}_2}{6\Delta t K_{3/2} + \rho_i h_i C}. \quad (15)$$

Substituting (6) and (15) into (12) gives $A_1 T_1^2 + B_1 T_1 + C_1 = 0$, where

$$A_1 \equiv \frac{\rho_i h_i}{2\Delta t} C + K_{3/2} \frac{4\Delta t K_{3/2} + \rho_i h_i C}{6\Delta t K_{3/2} + \rho_i h_i C} + \frac{K_{1/2} B}{K_{1/2} + B}, \quad (16)$$

$$\begin{aligned} B_1 \equiv -\frac{\rho_i h_i}{2\Delta t} \left(C \hat{T}_1 - \frac{L\mu S}{\hat{T}_1} \right) - I \\ - K_{3/2} \frac{4\Delta t K_{3/2} T_f + \rho_i h_i C \hat{T}_2}{6\Delta t K_{3/2} + \rho_i h_i C} + \frac{A K_{1/2}}{K_{1/2} + B}, \end{aligned} \quad (17)$$

and

$$C_1 \equiv -\frac{\rho_i h_i}{2\Delta t} L \mu S. \quad (18)$$

¹ All of the solar radiation that is absorbed by the ice is absorbed in the upper layer. However, some of the penetrating solar may pass through the ice to the ocean below. Indeed, it is desirable that a fraction, $\exp[-(h_o)/2h_o]$ where h_o is the ice optical depth, of the penetrating solar pass through the ice so that the thermal forcing of thin ice does not become so great that temperatures above the melting temperature are predicted. This approach is taken by Bettge et al. (1996) in their use of the Semtner model.

This is solved for T_1 , which is subsequently used in (15) to find T_2 and in (6) to find T_s . If this calculation gives a temperature greater than the melting temperature of snow (if there is snow cover) or sea ice (if there is none), the temperatures are recalculated using quadratic coefficients appropriate for the problem with the surface temperature fixed at freezing ($T_s = 0^\circ\text{C}$ when there is snow; $T_s = -\mu S$, the melting temperature of sea ice, when there is no snow):

$$A_1 \equiv \frac{\rho_i h_i}{2\Delta t} C + K_{3/2} \frac{4\Delta t K_{3/2} + \rho_i h_i C}{6\Delta t K_{3/2} + \rho_i h_i C} + K_{1/2}, \quad (19)$$

$$B_1 \equiv -\frac{\rho_i h_i}{2\Delta t} \left(C\hat{T}_1 - \frac{L\mu S}{\hat{T}_1} \right) - I - K_{3/2} \frac{4\Delta t K_{3/2} T_f + \rho_i h_i C\hat{T}_2}{6\Delta t K_{3/2} + \rho_i h_i C} - K_{1/2} T_s, \quad (20)$$

and C_1 is unchanged.

To summarize the ice temperature time-stepping procedure: The new upper ice temperature is given by

$$T_1 = -\frac{B_1 + (B_1^2 - 4A_1 C_1)^{1/2}}{2A_1}, \quad (21)$$

where A_1 , B_1 , and C_1 are given by (16)–(18). The new lower ice temperature is then given by (15) and the surface temperature by (6). If the surface temperature is greater than the freezing temperature of snow (when there is snow cover) or sea ice (when there is none), the surface temperature is fixed at the melting temperature of snow or sea ice, respectively, and the upper ice temperature is recomputed from (21) using the coefficients given by (19), (20), and (18). Then, T_2 is recomputed from (15) and an energy flux,

$$M_s = K_{1/2}(T_1 - T_s) - (A + BT_s) \quad (22)$$

is applied toward surface melting (thereby balancing the surface energy budget). Likewise, the energy for bottom melting (or freezing, if negative),

$$M_b = F_b - 4K_i(T_f - T_2)/h_i, \quad (23)$$

serves to balance the difference between the oceanic heat flux to the ice bottom F_b and the conductive flux of heat upward from the bottom.

b. Calculation of ice and snow mass changes

In addition to calculating ice temperature changes, the ice model must also readjust the sizes of the snow and ice layers 1) to accommodate mass fluxes at the upper and lower surfaces, 2) to convert snow below the waterline to ice, and 3) to equalize the thickness of the two ice layers. It is convenient to apply mass-increasing changes first. Snow is added to the snow layer and ice from two sources is added to the bottom layer. The first source is freezing at the ice–ocean interface from (23)

when M_b is negative. In this case, the bottom layer thickness h_2 (initially, $h_2 = h_1 = h_i/2$) is increased by

$$\Delta h_2 = M_b \Delta t / E_2(T_f, S), \quad (24)$$

where

$$E_2(T, S) \equiv C(T + \mu S) - L \quad (25)$$

is the enthalpy of the lower, fixed heat capacity, ice. Notice that, even though it does not contain brine, the lower ice has the melting temperature of saline ice. Frazil from the ocean mixed layer, possibly formed to balance heat fluxes through leads when the mixed layer temperature falls to seawater freezing temperature, is added to the bottom of the ice along with the portion frozen at the ice–ocean interface. Both are added at seawater freezing temperature, changing the lower layer temperature to

$$T_{2\text{new}} = \frac{(\Delta h_2 T_f + h_2 T_2)}{(\Delta h_2 + h_2)}. \quad (26)$$

Following, positive mass changes to the snow and ice layers, surface and bottom melting is applied. The surface melting that occurs to balance the (upper) surface energy budget described above reduces the snow thickness by

$$\Delta h_s = -\min \left\{ \frac{M_s \Delta t}{L}, h_s \right\}, \quad (27)$$

the upper ice thickness by

$$\Delta h_1 = -\min \left\{ \max \left[\frac{M_s \Delta t - L h_s}{-E(T_1, S)}, 0 \right], h_1 \right\}, \quad (28)$$

and the lower ice thickness by

$$\Delta h_2 = -\min \left\{ \max \left[\frac{M_s \Delta t - L h_s + E(T_1, S) h_1}{-E_2(T_2, S)}, 0 \right], h_2 \right\}. \quad (29)$$

An excess melt energy of

$$\max[M_s \Delta t - L h_s + E(T_1, S) h_1 + E_2(T_2, S) h_2, 0] \quad (30)$$

is applied to the ocean mixed layer. Similarly, if M_b is positive (bottom melting), the bottom ice thickness is reduced by

$$\Delta h_2 = -\min \left\{ \frac{M_b \Delta t}{-E_2(T_2, S)}, h_2 \right\}, \quad (31)$$

the upper ice thickness by

$$\Delta h_1 = -\min \left\{ \max \left[\frac{M_b \Delta t + E_2(T_2, S) h_2}{-E(T_1, S)}, 0 \right], h_1 \right\}, \quad (32)$$

and the snow thickness by

$$\Delta h_s = -\min \left\{ \max \left[\frac{M_b \Delta t + E_2(T_2, S)h_2 + E(T_1, S)h_1}{L}, 0 \right], h_s \right\}, \quad (33)$$

with excess melt energy of

$$\max[M_b \Delta t - Lh_s + E(T_1, S)h_1 + E_2(T_2, S)h_2, 0] \quad (34)$$

applied to the ocean mixed layer.

After the above adjustments have been made to the thickness of the snow and ice layers, two internal adjustments are made. The first converts snow below the waterline

$$\Delta h_s = -\max \left[\left(h_s - \frac{\rho_w - \rho_i}{\rho_s} h_i \right) \frac{\rho_i}{\rho_w}, 0 \right] \quad (35)$$

into upper layer ice

$$\Delta h_1 = \max \left[\left(h_s - \frac{\rho_w - \rho_i}{\rho_s} h_i \right) \frac{\rho_s}{\rho_w}, 0 \right], \quad (36)$$

where ρ_w is the density of seawater. Now the temperature of the upper ice layer must be adjusted to account for the incorporation of zero-heat-capacity snow. This is done based upon enthalpy conservation, that is, by determining the temperature of the new upper layer that gives an enthalpy equal to the average enthalpies of the old upper layer and the added snow. For this purpose we note that the snow enthalpy, $-L = E_2(-\mu S, S)$. Hence an expression for new upper ice temperature when adding lower-layer ice can also be used for adding snow simply by replacing T_2 with $-\mu S$. We now derive this expression that will also be used below for evening the ice layers.

Using (1) and (25) we can write the enthalpy of a new upper layer formed from a fraction f_1 of upper ice and $1 - f_1$ of lower ice,

$$E(T_{1\text{new}}) = f_1 E(T_1) + (1 - f_1) E_2(T_2). \quad (37)$$

Solving for this for $T_{1\text{new}}$ gives

$$T_{1\text{new}} = \frac{\bar{T} - (\bar{T}^2 + 4\mu S L/C)^{1/2}}{2}, \quad (38)$$

where

$$\bar{T} \equiv f_1 \left(T_1 - \frac{L \mu S}{C T_1} \right) + (1 - f_1) T_2. \quad (39)$$

The final adjustment evens the upper and lower layers of ice to maintain the layer structure depicted in Fig. 1. When shifting mass between the two layers, the temperature of the donating layer remains unchanged, while the temperature of the receiving layer is determined from averaging the enthalpies of the two ice

portions. Equation (38) is used for determining the new temperature of an upper layer when lower-layer ice is added to it. Averaging enthalpies for a new lower layer formed from a fraction f_1 of upper-layer ice and $1 - f_1$ of lower-layer ice gives a new lower layer temperature,

$$T_{2\text{new}} = \bar{T}, \quad (40)$$

where \bar{T} is given by (39).

When upper-layer ice is converted to lower-layer ice it is possible for the new lower layer temperature to exceed the ice melting temperature, $-\mu S$. A number of adjustments might be made to avoid this condition. In a coupled atmosphere–ice model at the Geophysical Fluid Dynamics Laboratory (GFDL), this extra sensible energy has been used to melt equal thicknesses from the upper and lower layers with good results.

3. Comparison to Semtner's model

To compare the new model with Semtner's model both were forced with climatological seasonal fluxes of downward short- and longwave radiation, and sensible and latent heat fluxes. The values used were the same used by Semtner to compare his model with the Maykut and Untersteiner model. As in Semtner (1976), the upward longwave was calculated using the Stefan–Boltzmann relation, and upward shortwave by applying a surface albedo. Rather than using the observed albedos, however, snow was given an albedo of 0.8—reduced to 0.75 under melting conditions—and ice an albedo of 0.65. The latter value was tuned to give an annual mean ice thickness of 3 m. The ocean heat flux to the ice was neglected.

Figure 2 shows the seasonal variation of snow, ice, brine, and temperatures for the two models. For 30% penetrating radiation and a salinity of 1 per mil in the new model, there is close agreement between the two models in the simulation of all properties. The differences are not significant since the ice salinity for new model was chosen to produce agreement between the models with a round number. The surface temperatures predicted by the models (not shown) were virtually identical. When the salinity is increased in the new model, the agreement with the Semtner model ice thickness and surface temperature remain, but the internal temperatures show a relative seasonal lag and decrease in seasonal amplitude. Figure 3 shows the annual mean ice thickness of the two models with a range of settings for

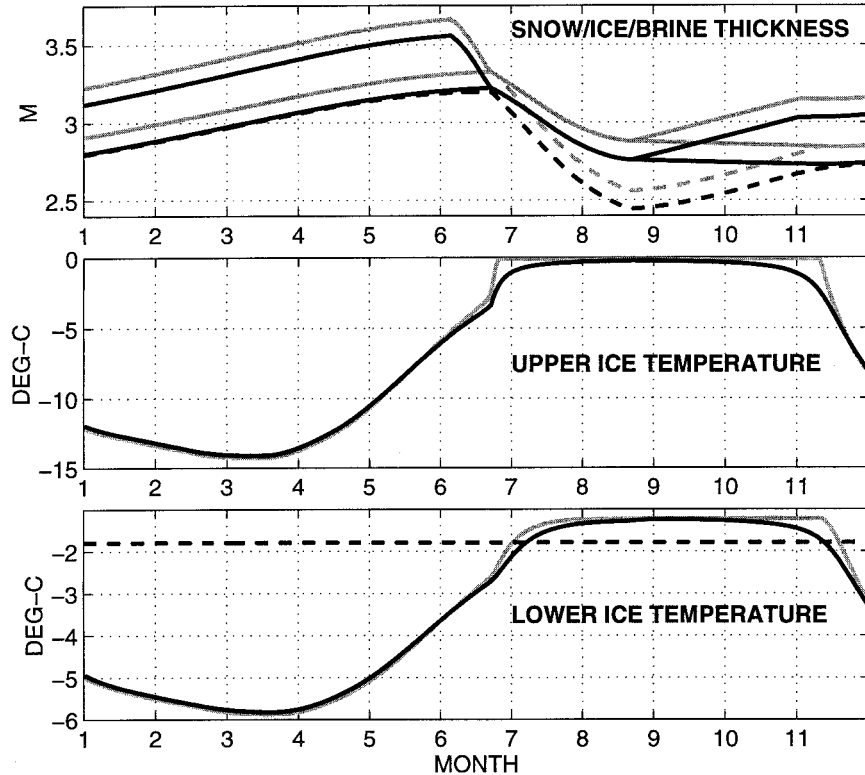


FIG. 2. Comparison of the new model with Semtner's model under climatological seasonal forcing. The new model results are depicted in black, Semtner model in gray. At top, snow is between the upper two solid lines, the lower solid line is the ice thickness, and the dashed line is the thickness of solid ice (i.e., the space between the dashed and solid line is the equivalent ice thickness bound up in brine pockets). The middle plot shows the upper ice temperatures for the two models. The lower plot shows the lower ice temperatures. The dashed line is the fixed bottom temperature of the ice. When the lower ice temperature is above this line there is melting at the bottom, when it is below, there is freezing.

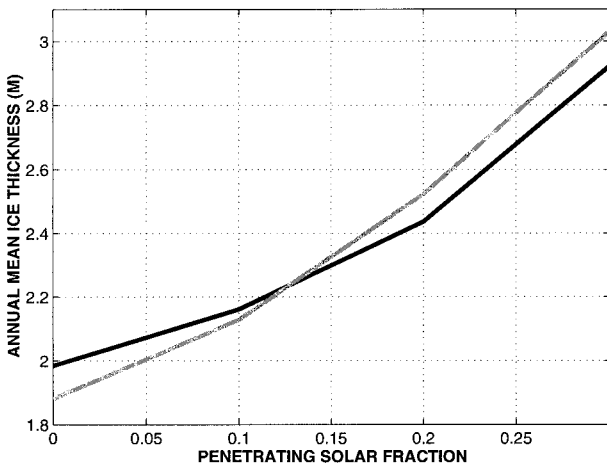


FIG. 3. Seasonal mean ice thickness in the new (black) and Semtner (gray) models with various settings for penetrating solar fraction. New model results are shown for an ice salinity of 1 per mil.

the fraction of solar radiation allowed to penetrate the ice. The sensitivity to this parameter is very similar for the two models. The new model has slightly less sensitivity due to having some storage of energy in brine pockets independent of the penetrating solar radiation (storage in brine pockets generally thickens the ice).

To compare the computational expense of the models, 1000 seasonal cycles of the above experiment were run on an SGI Indigo workstation and a Cray T90 supercomputer. The version of the Semtner model employed was that used as part of the National Center of Atmospheric Research CSM sea ice model (Bettge et al. 1996) available online at <http://www.cgd.ucar.edu:80/CCR/bettge/ice/>. The new model used 17% less CPU time on the SGI and 37% less CPU time on the Cray.

4. Conclusions

A reformulated three-layer sea ice model has been presented in this paper. This model offers several modest improvements over the widely used Semtner three-layer model. The upper ice layer is given a variable heat capacity putting the treatment of brine pockets on a firmer

physical footing than in the Semtner model—although the Semtner and new models simulate similar seasonal cycles for a particular choice of ice salinity in the new model. The new model is fully implicit, allowing longer time steps and eliminating the need to use a zero-heat-capacity model when the ice becomes thin. The new ice model has been coupled to an atmospheric model at GFDL and runs stably without any limitation upon ice thickness. Finally, the new model is somewhat more computationally efficient than Semtner's original model and carries fewer prognostic variables.

A FORTRAN code for the model described in this paper is available online at <http://www.gfdl.gov/~mw/>.

Acknowledgments. The author thanks Steve Griffies and Bob Hallberg for reviews of an early draft. Cecilia Bitz, Bill Lipscomb, and two anonymous reviewers made helpful comments leading to significant improvement of the paper.

REFERENCES

- Battisti, D. S., C. M. Bitz, and R. E. Moritz, 1997: Do general circulation models underestimate the natural variability in the Arctic climate? *J. Climate*, **10**, 1909–1920.
- Bettge, T. W., J. W. Weatherly, W. M. Washington, D. Pollard, B. P. Briegleb, and W. G. Strand Jr., 1996: The NCAR CSM Sea Ice Model. NCAR Tech. Note TN-425+STR, 25 pp. [Available from NCAR, P.O. Box 3000, Boulder, CO 80307-3000.]
- Bitz, C. M., and W. H. Lipscomb, 1999: A new energy-conserving sea ice model for climate study. *J. Geophys. Res.*, **104**, 15 669–15 677.
- , D. S. Battisti, R. E. Moritz, and J. A. Beesley, 1996: Low-frequency variability in the arctic atmosphere, sea ice, and upper-ocean climate system. *J. Climate*, **9**, 394–408.
- Ebert, E. E., and J. A. Curry, 1993: An intermediate one-dimensional thermodynamic sea ice model for investigating ice–atmosphere interactions. *J. Geophys. Res.*, **98**, 10 085–10 109.
- Eicken, H., H. Fischer, and P. Lemke, 1995: Effects of the snow cover on Antarctic sea ice and potential modulation of its response to climate change. *Ann. Glaciol.*, **21**, 369–376.
- Hibler, W. D., and G. M. Flato, 1992: Sea ice models. *Climate System Modeling*, K. Trenberth, Ed., Cambridge University Press, 413–436.
- Maykut, G. A., and N. Untersteiner, 1971: Some results from a time-dependent thermodynamic model of sea ice. *J. Geophys. Res.*, **76**, 1550–1575.
- Ono, N., 1967: Specific heat and heat of fusion of sea ice. *Physics of Snow and Ice*, H. Oura, Ed., Vol. I, Institute of Low Temperature Science, 599–610.
- Semtner, A. J., 1976: A model for the thermodynamic growth of sea ice in numerical investigations of climate. *J. Phys. Oceanogr.*, **6**, 27–37.